

# Semi-intrinsic self-healing performance of liquid-cored microcapsules in epoxy matrix

Cagatay Yilmaz<sup>1,2,3</sup>  | Mehmet Yildiz<sup>1,2,3</sup>  | Yusuf Menceloglu<sup>1,2,3</sup>

<sup>1</sup>Faculty of Engineering and Natural Sciences, Sabanci University, Tuzla, Istanbul, Turkey

<sup>2</sup>Integrated Manufacturing Technologies Research and Application Center, Sabanci University, Tuzla, Istanbul, Turkey

<sup>3</sup>Composite Technologies Center of Excellence, Istanbul Technology Development Zone, Sabanci University-Kordsa Global, Pendik, Istanbul, Turkey

## Correspondence

Mehmet Yildiz, Composite Technologies Center of Excellence, Istanbul Technology Development Zone, Sabanci University-Kordsa Global, Pendik, Istanbul, Turkey.  
Email: meylidiz@sabanciuniv.edu

## Abstract

We present an experimental study on the microcapsule-based semi-intrinsic self-healing behavior of low viscosity epoxy resin used in Resin Transfer Molding (RTM) process. The microcapsules containing RTM epoxy resin are prepared using in situ polymerization of urea-formaldehyde. Single type of microcapsules with six different agitation rates is prepared, resulting in microcapsules with a mean diameter ranging from 52 to 202  $\mu\text{m}$ . The thermal characteristics of each microcapsule batch are investigated using Differential Scanning Calorimetry (DSC) and Simultaneous Thermal Analysis (STA). In addition to thermal characterization tools, Fourier Transform Infrared Spectroscopy (FTIR) is also used as a qualitative technique to determine the composition of microcapsules. The mechanical properties of the self-healing specimen such as Mode-I fracture toughness and flexure strength are assessed by a universal testing machine, and the obtained results are compared with the findings in literature.

## KEYWORDS

in situ polymerization, microcapsules, mode-I fracture toughness, self-healing

## 1 | INTRODUCTION

Microcapsules with different active core materials have received a great deal of attention for developing polymer-based materials with self-healing abilities.<sup>[1–4]</sup> Once incorporated into polymeric host materials not only can microcapsules enable self-healing but also they can operate as toughening agents.<sup>[5,6]</sup> The self-healing literature focuses mostly on the healing of epoxy matrix as a host material, since epoxy resin is a very commonly used matrix material because of its unique mechanical properties for manufacturing composite materials. Cured resin holds fiber reinforcements together and protects them from mechanical and environmental damages as well as transfer the applied external load between reinforcements. The self-healing ability is crucial in particular for matrix materials having a brittle nature such as epoxy, wherein the cross-linked three-dimensional polymer chains do not allow for the reorientation of polymer chains. More

specifically, when a highly cross-linked polymer is exposed to a critical force, polymer chains crack because of the inability of the chain movement. On a micro scale, these cracked polymer chains in essence contribute to the formation of microcracks which may promote premature failure, hence leading to undesired results for structural polymeric materials. In order to abstain from an abrupt failure of structural brittle manner polymeric materials, microcapsules can be an excellent viable repair agent.

After the first successful self-healing study with the DCPD/Grubbs<sup>[3]</sup> catalyst system, several attempts were surfaced<sup>[7–10]</sup> to create a feasible self-healing systems for real structural application. Due to the several drawbacks of the DCPD/Grubbs such that Grubb's catalyst is rather expensive and degraded by the amine-based catalyst of matrix, it is important to develop sustainable and cost-effective self-healing materials where Grubb's catalyst is replaced by a new catalyst system. The second shortcoming of this system is the

DCPD itself, which is encapsulated by urea-formaldehyde and then the resultant microcapsules are incorporated into the host material. During the service of a structure made of self-healing composites, an incoming crack ruptures the shell of microcapsule whereby the stored DCPD in the microcapsule is released along with its vapor. It is known that the vapor of the unpolymerized DCPD may cause severe health problems to people in the vicinity of the component.<sup>[11]</sup>

To this end, the research on the microcapsule-based self-healing materials has recently focused on the encapsulation of diglycidyl ether of bisphenol-A (DGEBA) or commonly referred to as epoxy resin and its hardener (amine-based curing agent). The encapsulation of epoxy resin is achieved by several groups in literature by using the principle of in situ polymerization of urea-formaldehyde.<sup>[12,13]</sup> Nevertheless, a few studies have a limited success on the encapsulation of amine-based catalyst,<sup>[9,14]</sup> since the amine-based hardener system is water soluble and hence cannot be encapsulated by applying the procedure of the in situ polymerization of urea-formaldehyde. McIlroy et al.<sup>[14]</sup> attempted to encapsulate amine-based catalyst by using an inverse emulsion technique. Although the encapsulation was relatively successful, in their work, the assessment of healing was not presented, and McIlroy et al.<sup>[14]</sup> also pointed out that the encapsulation of amine in the water in oil emulsion technique was rather challenging to achieve. However, Jin et al.<sup>[9]</sup> developed an interesting procedure to encapsulate this water miscible catalyst. This method was based on producing hollow microcapsules and then impregnating them into a vacuumed jar containing amine in liquid phase. Although the efficiency of the vacuum infiltration system was low, the encapsulation of water soluble phase by the urea-formaldehyde was achieved. Jin et al.<sup>[9]</sup> incorporated both amine and epoxy microcapsules to a host material and their dual microcapsule system showed an average 91% recovery of mode-I fracture toughness value for a specimen cured at a low temperature. When specimens were post-cured at 120°C for 1 hr, the healing efficiency decreased drastically to 46% and 35% after 8 hr post-curing. The drop of healing performance was attributed to the diffusion of amine from the capsules at elevated temperature.

Different self-healing route and healing agents have been explored recently. For instance, Monfared Zanjani et al.<sup>[15]</sup> examined the self-healing of the tri-axial electro-spun fiber filled with both epoxy and hardener. Wang et al.<sup>[16]</sup> investigated the self-healing functionality of bitumen base material containing microcapsules used in pavement. Yi et al.<sup>[17]</sup> demonstrated the self-healing of anti-corrosion coating containing microcapsules filled with isophorone diisocyanate. Tan et al.<sup>[18]</sup> studied the self-healing performance of concrete with microcapsules containing silica solution.

To investigate the practicality and the feasibility of single microcapsule-based self-healing system without second

catalyst phase which is described as semi-intrinsic, we have only incorporated DGEBA-loaded microcapsules into the epoxy matrix. In our system, a second catalyst phase for hardening purpose of self-healing solution is not inserted, instead of the unreacted catalyst found in the matrix is used as self-healing catalyst. Liquid epoxy resin was encapsulated by urea-formaldehyde. A tapered double cantilever beam (TDCB) was used to assess the healing efficiency of a single microcapsule-based self-healing system.

## 2 | EXPERIMENTS

### 2.1 | Synthesis of microcapsules

Microcapsules containing an oily phase were produced by using in situ polymerization of urea-formaldehyde, following the method defined by Blaiszik et al.<sup>[7]</sup> The microcapsules store the mixture of Diglycidyl Ether of Bisphenol-A (DGEBA) (from Huntsman) and chlorobenzene (PhCl) (from Merck). Due to the relatively high viscosity of the core compound ( $\eta_{\text{DGEBA}} = 1.3 \text{ Pa s}$ ), the encapsulation of DGEBA alone by urea-formaldehyde in water is not possible. Therefore, PhCl, a non-polar solvent with a rather low viscosity value ( $\eta_{\text{PhCl}} = 0.75 \times 10^{-3} \text{ Pa s}$ ), was used to decrease the viscosity of DGEBA, thereby enabling its encapsulation. Figure 1a shows the micro-encapsulation setup, while Figure 1b schematically illustrates stages of microcapsule processing, which includes the following steps. Initially, 100 ml deionized water and 25 ml 1.5% wt/v aqueous solution of ethylene maleic anhydride copolymer (EMA) (from Vertellus), which acts as a surfactant, were mixed in a 250 ml beaker at room temperature. Having placed the beaker in a temperature controlled silicon oil bath with an external thermocouple (Velp Scientica Magnetic Stirrer and Digital Thermoregulator), the solution was agitated with a programmable digital mixer (Heidolph RZR 2102). As agitation continues, the wall material composed of 2.5 g  $\text{CO}(\text{NH}_2)_2$  (urea) (from Sigma-Aldrich), 0.25 g  $\text{NH}_4\text{Cl}$  (ammonium chloride) (from Sigma-Aldrich), and 0.25 g  $\text{C}_6\text{H}_6\text{O}_2$  (resorcinol) (from Carl Roth) was added to the solution. After the wall material is dissolved in the solution, approximately 15 min later, the pH of the solution was measured to be approximately 2.7 and then was raised to 3.5 through the drop-wise addition of the NaOH (sodium hydroxide). Before the addition of the core material, 15 ml DGEBA and 15 ml PhCl were mixed in a 50 ml beaker to decrease the viscosity of DGEBA to the desired viscosity range for the encapsulation, and the 30 ml DGEBA + PhCl mixture was very slowly added to the solution being agitated, forming a fine emulsified dispersed phase. To attain dispersed phase with uniform diameter by the help of EMA, the emulsion was stirred for additional 15 min. Subsequently, 6.68 g formalin (aqueous solution with 35% wt formaldehyde, purchased from Carlo Erba Reagents) was

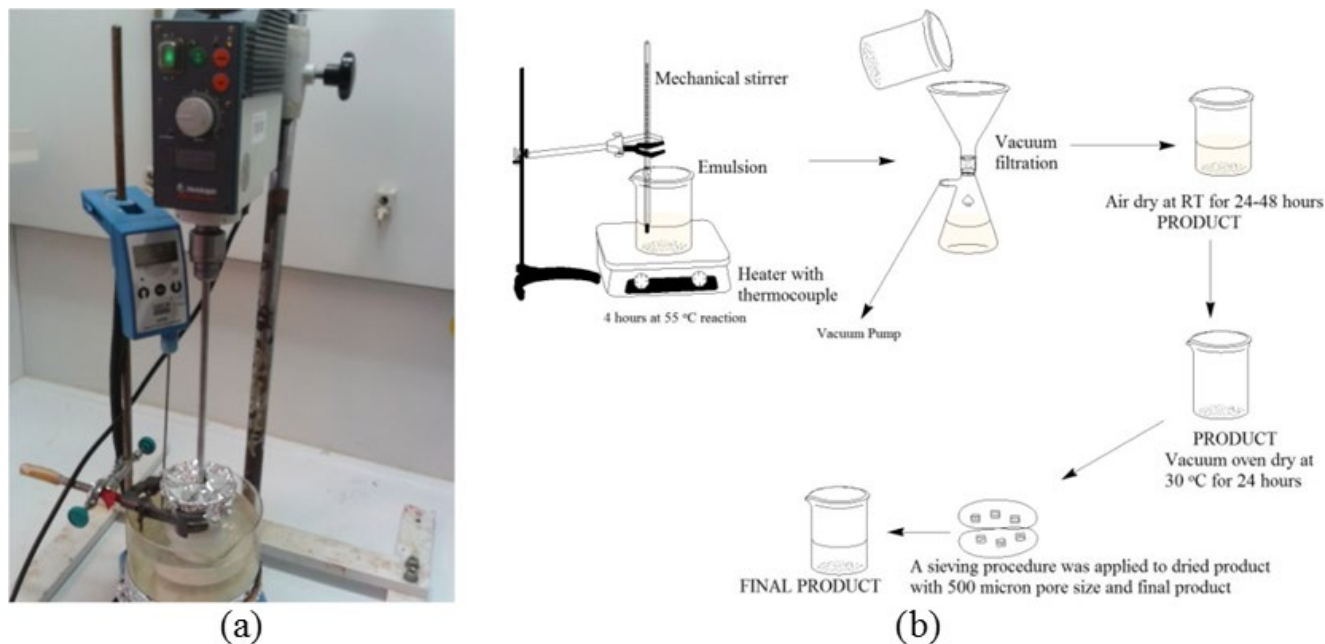


**FIGURE 1** (a) Micro-encapsulation setup, (b) processing chart of microcapsules involving the encapsulation reaction of diglycidyl ether of bisphenol-A (DGEBA), filtering of microcapsules from aqueous medium, air-dry, drying in vacuum oven to remove excess water, sieving with 500  $\mu\text{m}$  sieve, and final product [Color figure can be viewed at [wileyonlinelibrary.com](http://wileyonlinelibrary.com)]

added to the emulsion to initiate the formation of solid wall. It is noted that the molar ratio between formaldehyde and urea is calculated to be 1:1.9, which is reported to be an optimum ratio for which all reactants are consumed during the chemical reaction.<sup>[19]</sup> The beaker containing the emulsion was covered with an aluminum foil and then heated at a rate of  $1^\circ\text{C}/\text{min}$  up to  $55^\circ\text{C}$ . The reaction lasted for 4 hr with continuing agitation at  $55^\circ\text{C}$ , forming a suspension. One hundred milliliters of deionized water ( $55^\circ\text{C}$ ) was added to suspension to compensate for water loss during the synthesis. After the suspension cooled down to room temperature, the microcapsule slurry was filtered and washed several times with deionized water and dried in a fume hood for 36–48 hr. Then, it was dried in a vacuum oven at  $30^\circ\text{C}$  for 24 hr. Finally, the microcapsules were passed through a sieve of a 500- $\mu\text{m}$  hole size to get final microcapsules with a size smaller than 500  $\mu\text{m}$ .

## 2.2 | Thermal analysis

The thermal stability of each microcapsule batch was assessed by TGA (Netzsch STA 449 C). Approximately 30 mg of dried microcapsule powder was weighed from each batch in a ceramic crucible. The crucible was placed in a TGA. The sample was scanned in a controlled nitrogen atmosphere at  $10^\circ\text{C}/\text{min}$  ramp rate from a room temperature to  $500^\circ\text{C}$ , while mass loss trace was simultaneously recorded by software. Dynamic scanning calorimetry (DSC) experiments were conducted to measure heat flow of synthesized microcapsules from room temperature to  $350^\circ\text{C}$  in a nitrogen atmosphere at a heating rate of  $10^\circ\text{C}/\text{min}$ .

## 2.3 | Fourier Transform Infrared Spectroscopy analysis

The chemical bond analysis of all microcapsule batches and compounds of interest was done by using an IR spectrometer (Thermo Scientific Smart iTR Nicolet i510). The attenuated total reflectance (ATR) mode of the FTIR system was used. The background was collected from 32 scans between the ranges of  $500\text{--}4,000\text{ cm}^{-1}$  called as Mid-IR. When the background scan was completed, the tip of ATR unit was unclamped and microcapsules samples or compounds of interest were placed on the ATR crystal. After establishing the required conditions for Mid-IR measurement of microcapsules samples or compounds, the scan was initiated. A total of 32 scans were collected from each sample. The background was extracted and the Mid-IR spectra of each microcapsule batch or compounds were obtained.

## 2.4 | Size distributions

An optical microscope (Nikon ECLIPSE ME600) was used to take the optic images of urea-formaldehyde walled microcapsules containing a hydrophobic core material. All images were taken with either  $5\times$  or  $10\times$  magnifications. Small amounts of dried microcapsule powder were poured in a Petri dish containing mineral oil. A good dispersion of microcapsules in mineral oil was achieved by shaking the Petri dish several times. The mineral oil bath was used to separate the individual microcapsules from one other since microcapsules tend to stick together. By changing the location of the

Petri dish with a manual carrier, at least 100 microcapsule images were obtained from a different region of Petri dish for each batch. Microcapsules sizes were determined using the image analyses software (Spot Advanced Version 4.6). The mean microcapsule batch diameter was calculated for each microcapsule batch by finding the mean value of total measurements.

## 2.5 | SEM image of microcapsules and fracture surface

The surface morphology of microcapsules was examined by field emission scanning electron microscopy (FE-SEM, Gemini Leo-SUPRA 35VP). First, a carbon tape was mounted on a conductive stage, and then microcapsule samples were placed on the carbon tape. Microcapsules were sputtered with a thin layer of carbon in coater to prevent charging under accelerated electron beam. FE-SEM sample holder with microcapsule was placed on the FE-SEM stage. Images of the microcapsules were taken under different magnifications with an acceleration voltage rate of 2 kV. FE-SEM was also used to image fracture surface of TDCB samples with a 2–5 kV electron source after sputter coating with carbon or gold source. Images of fracture surface were taken with different magnifications and from different location of crack plane.

## 2.6. | Mechanical characterizations

To evaluate the healing efficiency of a single microcapsule-based self-healing system, a tapered double cantilever beam (TDCB) specimen as described by Brown et al.<sup>[20]</sup> was employed, since it enables crack length independent measurement of the fracture toughness of polymeric materials unlike Double Cantilever Beam (DCB). For brittle materials, such as the epoxy resin used in this work and tested by TDCB geometry, all the strain energy imposed by grips are consumed to propagate an existing crack. The self-healing efficiency is described as a ratio of healed fracture toughness value to virgin fracture toughness. Fracture toughness value  $K_{IC} = \alpha P_c$  of TDCB specimen is only dependent on a geometric constant  $\alpha$  and critical force  $P_c$  which is the force to propagate an existing pre-crack. To allow for the controlled crack growth mechanism, side grooves were created on the original geometry. The specimen thickness is  $b = 6.25$  mm outside of the crack plane and  $b_n = 2.5$  mm in the crack plane. The long edge of the specimen is 76.2 mm and the short edge of the specimen is 61 mm. The specimen's V-notch side grooves have an angle of  $45^\circ$  and the length of 59 mm. The thickness reduction in the crack plane is equal to 60% ( $b_n/b = 0.4$ ). The distance from the load line to the end of specimen is 79.3 mm. Technical drawing of TDCB specimen can be seen in Figure 2a. For the specimen used in this

work,  $\alpha = 11.2 \times 10^3 \text{ m}^{-3/2}$  for crack lengths varying from 20 to 40 mm.<sup>[21]</sup> The model geometry for the modified TDCB specimen was machined from Aluminum by a CNC machine tool. The middle section of the specimen where V-notch side grooves are located was manufactured by using a line erosion machine with the line diameter of 250  $\mu\text{m}$ . Upon using the Aluminum model of TDCB geometry, several silicon-rubber molds were manufactured. Molds were composed of two different parts. The first part was only utilized to produce the middle part of the TDCB sample where the microcapsules are present, while the second part was employed to create the whole TDCB specimen.

The host material is the mixture of the Huntsman LY 564/XB 3403, namely epoxy/polyoxyalkylene amine hardener system. The resin system is mixed with or without microcapsules with 20% weight percentages, degassed, and poured into the dedicated silicon mold. The self-healing part of the TDCB fracture specimen is cured at  $50^\circ\text{C}$  for 15 hr and then was placed into the silicone mold for manufacturing the whole TDCB specimen. The two-part resin system is prepared with the ratio of 100:36 by weight, degassed in a vacuum jar, and then poured into the silicone rubber mold. The sample is cured at  $50^\circ\text{C}$  for 15 hr. Note that while curing the TDCB fracture specimen, the middle part gets additional heat treatment at  $50^\circ\text{C}$  for 15 hr. A sharp pre-crack was gently introduced by custom-made apparatus that can be seen in Figure 2b. After introducing a pre-crack, the specimen was assembled with a special fixture for transferring load from the testing machine onto specimen and then tested with Zwick Z100 universal testing machine as shown in Figure 2c.

All the mechanical fracture experiments in this study were conducted under a static loading condition in which the samples were loaded monotonically. The rate of crosshead displacement was set to 5  $\mu\text{m/s}$  in tension mode to carry out fracture experiment in a quasi-static fashion, so that inertial force is negligible and all the mechanical energy is consumed to trigger fracture process. Fracture experiments were conducted on two different sets of samples, namely those with and without microcapsules in the central region of the TDCB specimen. The samples without any microcapsules were tested as control samples, while those with microcapsules in the crack plane were tested for studying the in situ self-healing mechanisms of the system of interest.

## 3 | RESULTS AND DISCUSSION

### 3.1 | Infrared spectrum of microcapsules

In this work, in addition to TGA and DSC traces, the Fourier Transform Infrared Spectroscopy (FTIR) was also used to determine the chemical structure of microcapsules. FTIR provides a time-saving method to determine the content

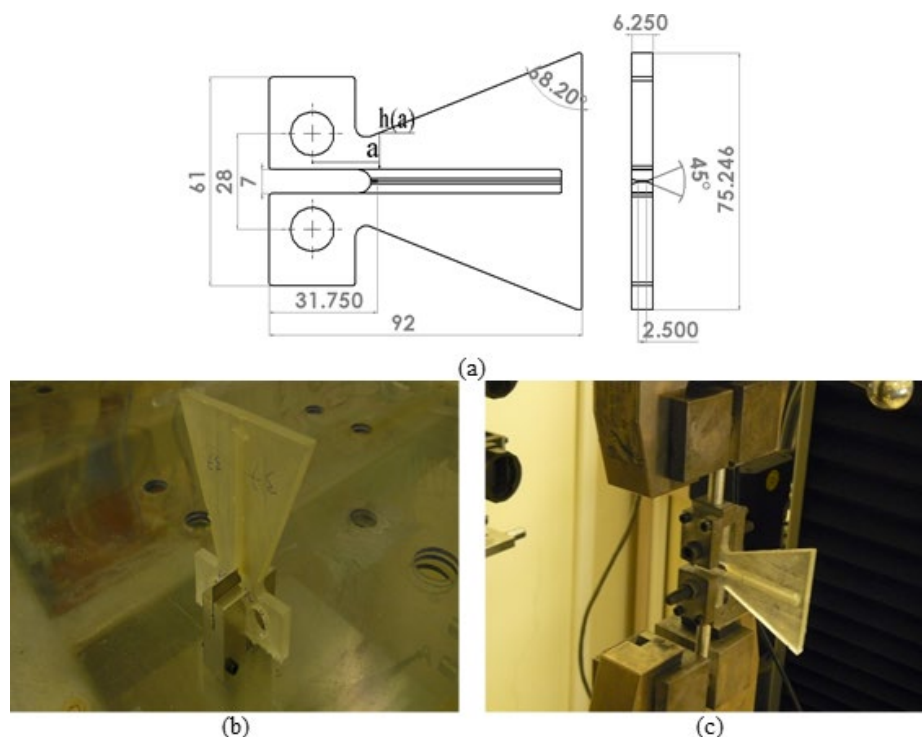


**FIGURE 2** (a) Basic dimension of tapered double cantilever beam (TDCB) specimen, (b) imposing pre-crack, and (c) mechanical testing [Color figure can be viewed at [wileyonlinelibrary.com](http://wileyonlinelibrary.com)]

of microcapsules without losing any material. The Mid-IR spectra of microcapsules prepared at different agitation rate can be seen in Figure 3a. Results can be summarized as follows: the C–H stretching of the epoxide group is around at  $3,055\text{ cm}^{-1}$ , indicating the encapsulation of DGEBA. C–O–C stretching vibration of the epoxide ring at  $829$  and  $914\text{ cm}^{-1}$  also indicates the existence of DGEBA in each microcapsule batches. The broad peak at  $3,325\text{ cm}^{-1}$  is the characteristic of –NH and –OH functional groups. NH and OH peaks prove formation of urea-formaldehyde cross-linked polymer around the core. One characteristic peak of chlorobenzene at the wavenumber  $740\text{ cm}^{-1}$  can be seen

in Figure 3a which is the C–Cl stretching of chlorobenzene. Figure 3a also indicates that microcapsules prepared at different agitation rates yield the same peak values on the wavenumber axis, which is an evidence for successful encapsulation of DGEBA by urea-formaldehyde polymer. Figure 3b shows Mid-IR spectra for urea-formaldehyde polymer prepared at  $467\text{ rpm}$  as a shell material, mixture of DGEBA–PhCl as a core material, and the microcapsule batch prepared at  $467\text{ rpm}$ . Figure 3b proves that microcapsules comprise of core (DGEBA + PhCl mixture) and shell (urea-formaldehyde polymer) material by having the characteristic Mid-IR peaks of its constituents.

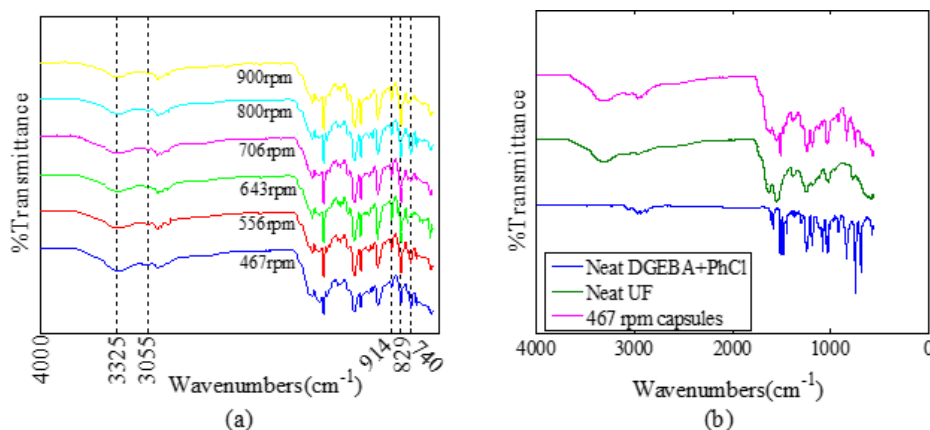


**FIGURE 3** Mid-IR spectra of (a) microcapsule batches prepared at different agitation rate, and (b) core, shell and a microcapsule batch prepared at  $467\text{ rpm}$  [Color figure can be viewed at [wileyonlinelibrary.com](http://wileyonlinelibrary.com)]

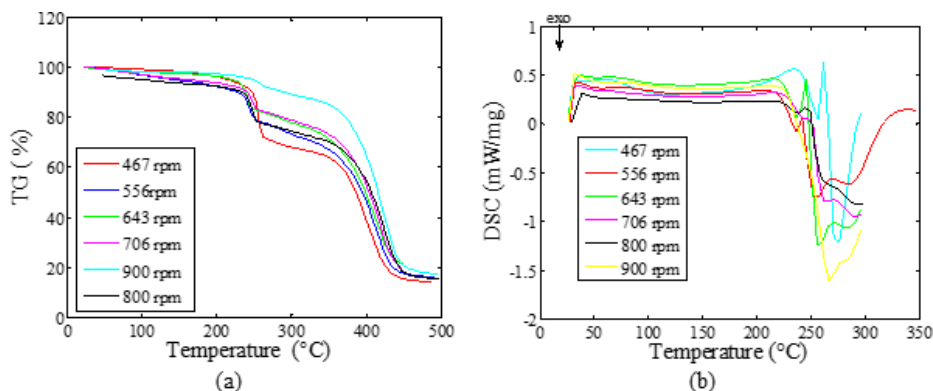


**FIGURE 4** (a) TGA trace of six different microcapsule batches prepared at different agitation rates, and (b) differential scanning calorimetry (DSC) trace of same microcapsule batches [Color figure can be viewed at [wileyonlinelibrary.com](http://wileyonlinelibrary.com)]

### 3.2 | Thermal characterization of microcapsules

The TGA trace of each microcapsule batches can be seen in Figure 4a. The mass loss around 240°C is due to the decomposition of the urea-formaldehyde shell wall. The point around 350°C is the decomposition temperature of DGEBA. By using the decomposition point of DGEBA on the TGA trace, the mass fraction of DGEBA can be obtained in each microcapsule sample. The amount of DGEBA in six different microcapsules batches is between 60% and 85%. DSC results of each microcapsule batch can be seen in Figure 4b. The endothermic peak at approximately 240°C corresponds to the decomposition temperature of urea-formaldehyde.<sup>[22]</sup> The exothermic one at about 261°C might be due to the rapid exothermic polymeric reaction of core material, which is triggered by the gaseous products such as ammonia, monomethylamine, and trimethylamine produced by the decomposition of shell materials.

### 3.3 | Visualization of microcapsules and effect of agitation rate

Optical microscope images in Figure 5 confirm the formation of microcapsules in addition to thermal and spectroscopic

characterization results. It is seen that microcapsules do not agglomerate in mineral oil medium (a non-polar material) and can be distinguished individually. One can infer that the microcapsules will also form a good dispersion in epoxy matrix due to the non-polar nature of epoxy. In Figure 5, the shell of the microcapsules appears to be black because of the difference in refractive indices of the shells of the microcapsules and that of mineral oil. However, due to the refractive index-matching of core and mineral oil, the centers of microcapsules have the same color as that of the mineral oil.

The SEM images in Figure 6 show that the outer surface of microcapsule shell has a rough morphology, which is due to the agglomeration of urea-formaldehyde particles. During the encapsulation of core material, urea-formaldehyde prepolymer forms and then precipitates on the surface of the core material as its molecular weight increases. As the reaction continues, more urea-formaldehyde pre-polymer precipitates, hence results in a rough surface of shell. The rough surface of the microcapsules enhances the adhesion between microcapsules and matrix by providing more surface areas.

During the synthesis of each microcapsule batches, the mean batch diameter is controlled by agitation rate, as seen in Figure 7. When the agitation rate increases, the mean diameter of microcapsule batches and its standard deviation decrease. This is related with shear force acting on the core

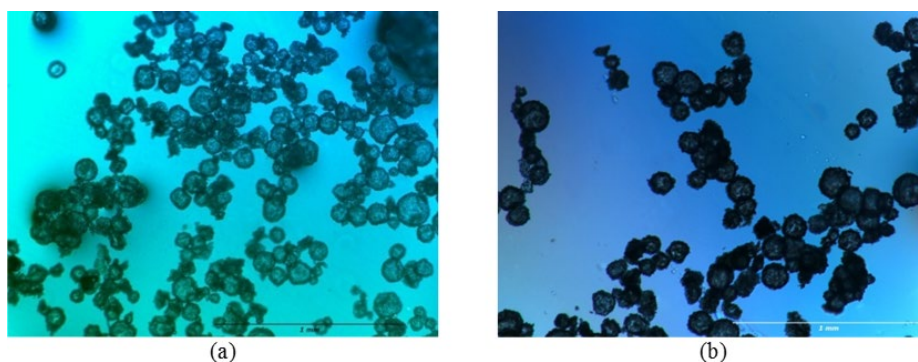


**FIGURE 5** (a and b) Optical microscope images of microcapsules [Color figure can be viewed at [wileyonlinelibrary.com](http://wileyonlinelibrary.com)]

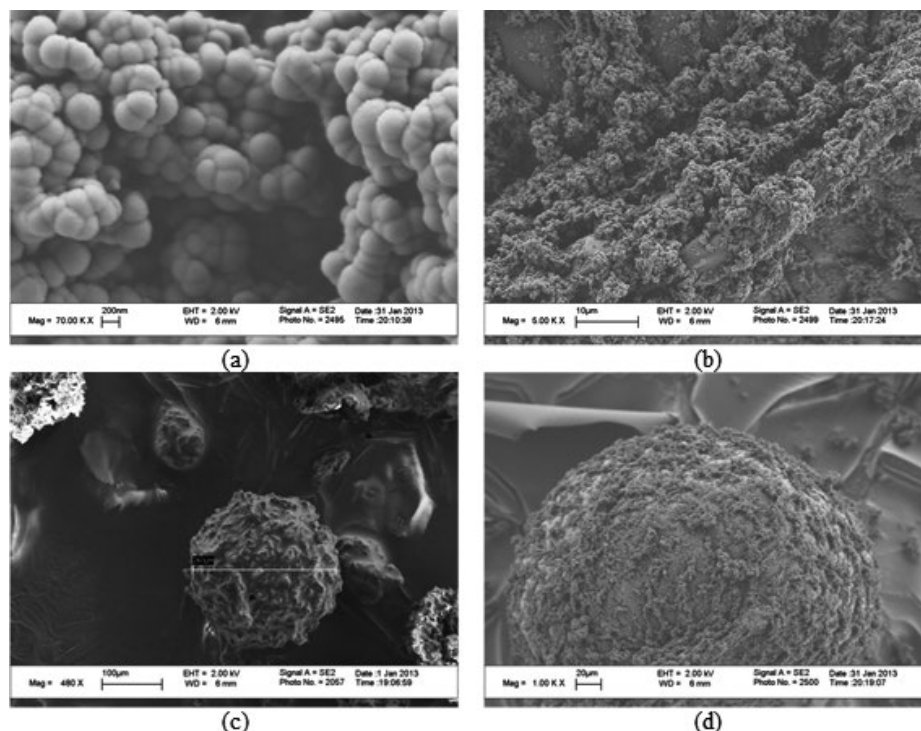


**FIGURE 6** SEM image of (a) a microcapsule outer surface (at 70 KX), (b) outer surface of same microcapsule (at 5 KX), (c) same microcapsule (at 480 X), and (d) another microcapsule

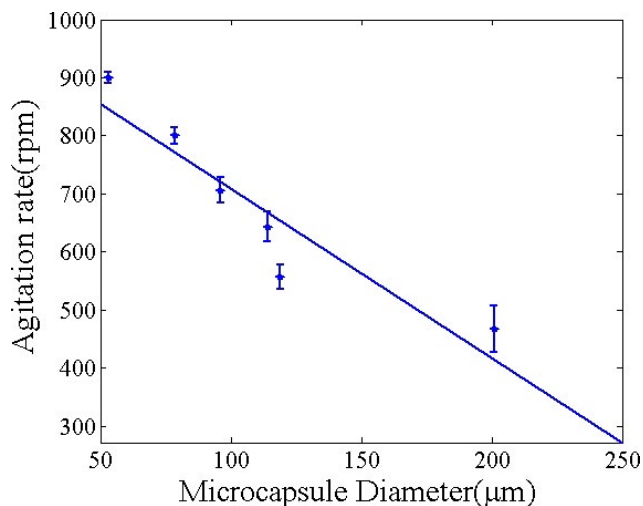


**FIGURE 7** Agitation rate versus mean batch diameter [Color figure can be viewed at [wileyonlinelibrary.com](http://wileyonlinelibrary.com)]

material. Namely, as the shear force increases, droplets (core materials) break up into new droplets with smaller diameters.

### 3.4 | Mechanical testing

In this semi-intrinsic self-healing approach, self-healing functionality of a host material is attained through curing of microencapsulated epoxy healing agent by a catalyst provided by unreacted amine groups in the host. As seen in Figure 2, a TDCB specimen with self-healing functionality is

pre-cracked and then subjected to tensile loading to propagate the crack front until the specimen breaks apart. Subsequently, two halves of TDCB specimen are brought together and kept in a furnace at 50°C for 24 hr for self-healing process. The crack propagation ruptures rather brittle wall of microcapsules whereby encapsulated healing agent leaks into the crack zone or plane and thus reacts with the unreacted amine groups in the host material. The local curing process in the vicinity of the crack zone takes place, leading to the repair of the damaged zone. A fracture plane of a self-healing sample can be seen in Figure 8a where circular indentations indicate ruptured microcapsules and thin flaky films confirm the polymerization of self-healing agent released by ruptured microcapsules in the crack plane upon loading. Similar polymerized films due to self-healing process of self-healing agents have also been documented by Brown et al.,<sup>[23]</sup> revealing that the self-healing method in this study is successful.

Being able to divulge the difference between fracture surfaces of specimens with and without self-healing capability, another TDCB specimen having microcapsules is broken apart and then both fracture surfaces of the TDCB specimen are wiped off to remove released healing agent. Therefore, the crack planes in Figure 8b are not covered by polymerized films of self-healing agent. The tails formed in the wake of the microcapsules as shown in Figure 8b is due to the crack pinning effect<sup>[24]</sup> of the microcapsules in fracture planes, which is evidenced by the increase in the mode-I fracture toughness of the host material as given in Table 1.

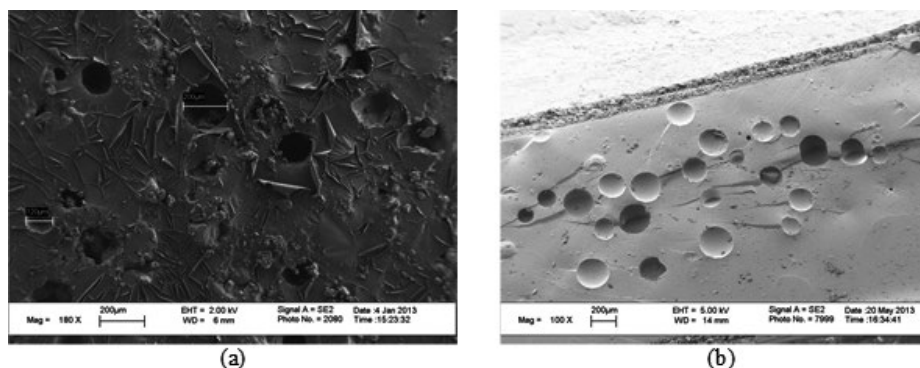


**FIGURE 8** SEM image of fracture surfaces: (a) a healed sample, (b) non-healed

**TABLE 1** Effect of microcapsules on the virgin tapered double cantilever beam (TDCB) peak load and fracture toughness  $K_{IC}$

	Virgin peak load (N)	$K_{IC}$ (MPam <sup>1/2</sup> )
Manufacturer		1.05
TDCB with neat epoxy	97	1.09
TDCB with microcapsules	129	1.44

Representative results of mode-I fracture tests are presented in Figure 9 where it is seen that the self-healed samples regain their structural integrity and strength albeit not being as high as the virgin structure, even though the samples are healed at relatively high temperatures for a long period of time. Due to the relatively high curing temperature of the host material, the amount of unreacted amine groups is lower. This results in the lack of catalyst in the crack plane, which decreases the healing efficiency of the intrinsic self-healing process.

The healing efficiency in the semi-intrinsic self-healing process is also influenced by high virgin fracture toughness value of the resin system employed in this study. The RTM resin system used here has a higher average fracture toughness value (1.09 MPam<sup>1/2</sup>) than that (0.55 MPam<sup>1/2</sup>) for the resin system (EPON 828/DET) of Brown et al.<sup>[20]</sup> Moreover, the current resin system has a critical load of 97 N at failure, while

EPON 828/DETA possesses a critical load of 49 N at failure. These differences also contribute to the healing efficiency difference between the current work and the literature.<sup>[20]</sup> The efficiency of the semi-intrinsic self-healing process can be improved through embedding catalyst-loaded microcapsules in the host material along with the healing agent loaded microcapsules. In this case, since incoming cracks would rupture both encapsulated the healing agent and the catalyst solution simultaneously, the lack of unreacted amine groups in the crack zone would be no longer a problem, and both healing agent and the catalyst would be able to react to initiate local cross-linking of healing solution in the crack plane.

The effect of microcapsule on the flexure strength of self-healing materials can be seen in Figure 10. Three different sets of epoxy-microcapsule composite sample with 20% microcapsule content were produced and tested in accordance with ASTM D 790 standard to investigate the effect of the microcapsules diameter on the flexural strength of composite. These experimental sets include microcapsules with different mean diameters, namely 180, 95, and 51  $\mu\text{m}$ , which are controlled through utilizing different agitation rates. For each set, five samples were tested to have a reliable averaged result. The flexure strength of the neat epoxy system was measured to be approximately 95 MPa. It is noted that the incorporation of microcapsules into the host material decreased its flexure strength, which might be attributed to the fact that micron

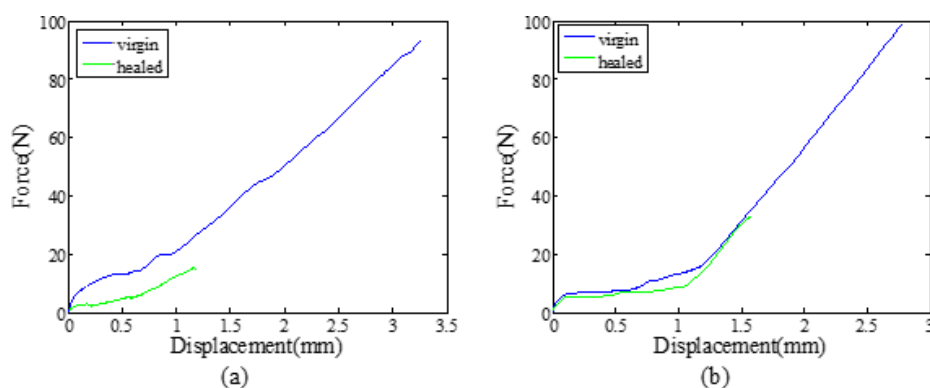


**FIGURE 9** Representative force-displacement curves for self-healing specimens [Color figure can be viewed at wileyonlinelibrary.com]

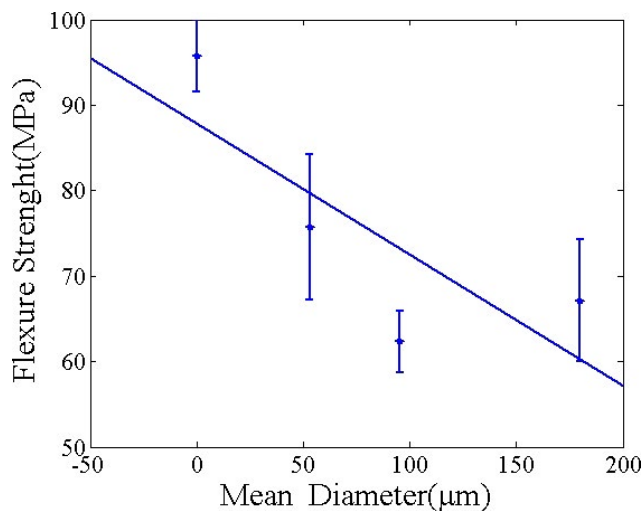


**FIGURE 10** Mean microcapsule diameter versus flexure strength [Color figure can be viewed at [wileyonlinelibrary.com](http://wileyonlinelibrary.com)]

size microcapsules act as crack initiation points or defects, hence decreasing the flexural performance of host material.

## 4 | CONCLUSION

Solvent-promoted DGEBA microcapsules were successfully produced by in situ polymerization of urea-formaldehyde on the water-emulsified phase interface. Their chemical characteristics were obtained by the Mid-IR spectrum. The thermal behavior of each microcapsule batches was evaluated by a thermogravimetric analyzer. The results indicated that microcapsules are thermally stable up to 250°C and, therefore, can be used for producing self-healing composites. The results of mode-I fracture toughness experiments indicated that the current healing system with micro capsules including only epoxy resin provides relatively low healing efficiency, which can be attributed to the unavailability of the unreacted catalyst in the crack plane. Thus, to have a higher healing efficiency, an excess amount of catalyst needs to be provided into the host separately to polymerize the released healing agent, which can be achieved by preparing microcapsules containing only catalyst.

## REFERENCES

- [1] M. Keller, N. Sottos, *Exp. Mech.* **2006**, *46*, 725.
- [2] M. M. Caruso, D. A. Davis, Q. Shen, S. A. Odom, N. R. Sottos, S. R. White, J. S. Moore, *Chem. Rev.* **2009**, *109*, 5755.

- [3] S. R. White, N. Sottos, P. Geubelle, J. Moore, M. R. Kessler, S. Sriram, E. Brown, S. Viswanathan, *Nature* **2001**, *409*, 794.
- [4] J. D. Rule, E. N. Brown, N. R. Sottos, S. R. White, J. S. Moore, *Adv. Mater.* **2005**, *17*, 205.
- [5] B. Blaiszik, N. Sottos, S. White, *Compos. Sci. Technol.* **2008**, *68*, 978.
- [6] J. D. Rule, N. R. Sottos, S. R. White, *Polymer* **2007**, *48*, 3520.
- [7] B. Blaiszik, M. Caruso, D. McIlroy, J. Moore, S. White, N. Sottos, *Polymer* **2009**, *50*, 990.
- [8] S. H. Cho, H. M. Andersson, S. R. White, N. R. Sottos, P. V. Braun, *Adv. Mater.* **2006**, *18*, 997.
- [9] H. Jin, C. L. Mangun, D. S. Stradley, J. S. Moore, N. R. Sottos, S. R. White, *Polymer* **2012**, *53*, 581.
- [10] D. M. Chipara, M. Flores, A. Perez, N. Puente, K. Lozano, M. Chipara, *Adv. Polym. Technol.* **2013**, *32*, E505.
- [11] *Dicyclopentadiene (DCPD)*, MSDS ID:NOVA-0006, NOVA Chemicals, Alberta, Canada **2014**.
- [12] S. Cosco, V. Ambrogio, P. Musto, C. Carfagna, *Macromol. Symposia* **2006**, *234*, 184.
- [13] T. S. Coope, U. F. Mayer, D. F. Wass, R. S. Trask, I. P. Bond, *Adv. Funct. Mater.* **2011**, *21*, 4624.
- [14] D. A. McIlroy, B. J. Blaiszik, M. M. Caruso, S. R. White, J. S. Moore, N. R. Sottos, *Macromolecules* **2010**, *43*, 1855.
- [15] J. S. Monfared Zanjani, B. S. Okan, I. Letofsky-Papst, Y. Menciloglu, M. Yildiz, *RSC Adv.* **2015**, *5*, 73133.
- [16] Y.-Y. Wang, J.-F. Su, E. Schlangen, N.-X. Han, S. Han, W. Li, *Constr. Build. Mater.* **2016**, *121*, 471.
- [17] H. Yi, Y. Yang, X. Gu, J. Huang, C. Wang, *J. Mater. Chem. A* **2015**, *3*, 13749.
- [18] N. P. B. Tan, L. H. Keung, W. H. Choi, W. C. Lam, H. N. Leung, *J. Appl. Polym. Sci.* **2016**, *133*, doi: 10.1002/app.43090.
- [19] P. Grad, R. Dunn, *Anal. Chem.* **1953**, *25*, 1211.
- [20] E. N. Brown, N. R. Sottos, S. R. White, *Exp. Mech.* **2002**, *42*, 372.
- [21] E. Brown, *The. J. Strain Anal. Eng. Des.* **2011**, *46*, 167.
- [22] L. Yuan, G.-Z. Liang, J.-Q. Xie, J. Guo, L. Li, *Polym. Degrad. Stab.* **2006**, *91*, 2300.
- [23] E. N. Brown, S. R. White, N. R. Sottos, *Compos. Sci. Technol.* **2005**, *65*, 2474.
- [24] R. A. Pearson, A. F. Yee, *Polymer* **1993**, *34*, 3658.

**How to cite this article:** Yilmaz C, Yildiz M, and Menciloglu Y. Semi-intrinsic self-healing performance of liquid-cored microcapsules in epoxy matrix. *Adv Polym Technol.* 2017;00:1–9. doi:10.1002/adv.21802.